PROCEEDINGS of the
23rd International Congress on Acoustics

9 to 13 September 2019 in Aachen, Germany

Statistical characteristics of Gas Metal Arc Welding (GMAW) sound

Sipei ZHAO[1]; Xiaojun QIU[1]; Ian BURNETT[1]; Malcolm RIGBY[2]; Anthony LELE[2]

[1] Centre for Audio, Acoustics and Vibration, Faculty of Engineering and IT, University of Technology Sydney, Australia

[2] Sound Intuition Ltd. Pty., Australia

ABSTRACT

Gas Metal Arc Welding (GMAW) is an arc welding process to join two or more metal materials through fusion, where an electric arc is formed between a consumable electrode and the base metal. It has been reported that expert GMAW welders can direct the welding arc type based on the welding sound, and psychoacoustic experiments show that the welding performance is significantly degraded without the acoustic feedback to the welders. In addition, identifying the metal transfer mode based on the welding sound is critical for automatic GMAW process monitoring, quality control and a training pathway for competency. However, the research on the generation and characteristics of the welding sound is still rare. In this paper, the welding sound is measured simultaneously with the welding current at different metal transfer modes to investigate the unique characteristics of welding sound. The welding sound consists of many impulses corresponding to the current leap. The envelope of the impulse responses is estimated based on the sound pressure signal for statistical analysis. It is found that the probability density function of the peak sound pressure, impulse interval and event duration can be well modelled by the Burr distribution. The findings can be used to classify the metal transfer mode from its welding sound.

Keywords: Welding Sound, GMAW, Arc

1. INTRODUCTION

Arc welding is used to join two or more materials through fusion so that the joint exhibits a sufficient strength and fracture toughness (1). Gas Metal Arc Welding (GMAW) is widely used in industry due to its high metal deposition and ease of automation with better weld quality (2). The acoustic emissions from a GMAW process contain information on the weld quality and can be utilized for online monitoring, inspection and quality control and training of welding processes.

The ultrasonic acoustic emission from welding was first measured to detect the defects in the weld (3). Saini and Floyd (1998) developed an online welding quality control system based on audible sound, where the time domain features were used to detect deviations from ideal arc while the frequency domain features showed some promise for metal transfer mode classification (4). Similarly, various time and frequency domain features have been explored for welding quality monitoring and control based on sound signals (5,6). In addition, different signal processing techniques have been utilized to enhance the welding sound signals for better robustness, such as the wavelet package transformation (7) and the Hilbert Huang transform (8).

In addition, advanced machine learning algorithms have also been used for GMAW process monitoring using welding sound signals (5). The random forest algorithm was used to classify 3 categories of welding quality, where the inputs for the decision tree algorithm were the statistical features extracted from the welding sound signals (9). The artificial neural network was employed for online welding quality monitoring, and a prediction rate of 80-90% for penetration degree was achieved based on training with a large data set (10). The Gaussian Mixture Model (GMM) was utilized to identify the metal transfer mode from the welding sound signals and a 10-fold cross validation shows a 90% accuracy (11).

In summary, the significance of acoustic sensing in monitoring the arc welding processes has been identified by many researchers. However, the existing research relies on general audio features,

[1] sipei.zhao@uts.edu.au

which are not dedicated for welding sound signals. In a different approach, this paper explores the unique statistical characteristics of the welding sound. The welding sound for different metal transfer modes is measured simultaneously with the welding current. The welding sound is found to consist of a sequence of impulse responses, each of which corresponds to a welding current pulse and metal droplet shape. The envelope of the impulse responses in the welding sound is estimated for statistical analysis. It is shown that the probability density function of the peak sound pressure, the impulse interval and the event duration obey the Burr distribution. The model parameters vary for the welding sound measured at different metal transfer modes, which is promising for automatic metal transfer mode classification in the future.

2. EXPERIMENTS

The experimental setup is illustrated in Figure 1. A Lincoln Electric PowerWave C300 welder was used in the experiments, where the torch was positive and the negative cable was connected to the work bench. During the welding, the torch was fixed and the work bench was moving, which was controlled by a servo motor and the travel speed could be set manually. A GRAS 40PH free field microphone was hanged 1.0 m above the weld pool to record the welding sound. The microphone was connected to an NI 9234 Sound and Vibration module. An LEM HTA 300-S current sensor was installed around the torch cable to measure the welding current through the torch. The current sensor was connected to an NI 9215 Analogue Voltage Input module. Both the NI 9234 and NI 9215 modules were installed in an NI cDAQ 9185 chassis, which was connected to a DELL Optiplex 7060 computer with a professional DELL P2918H monitor.

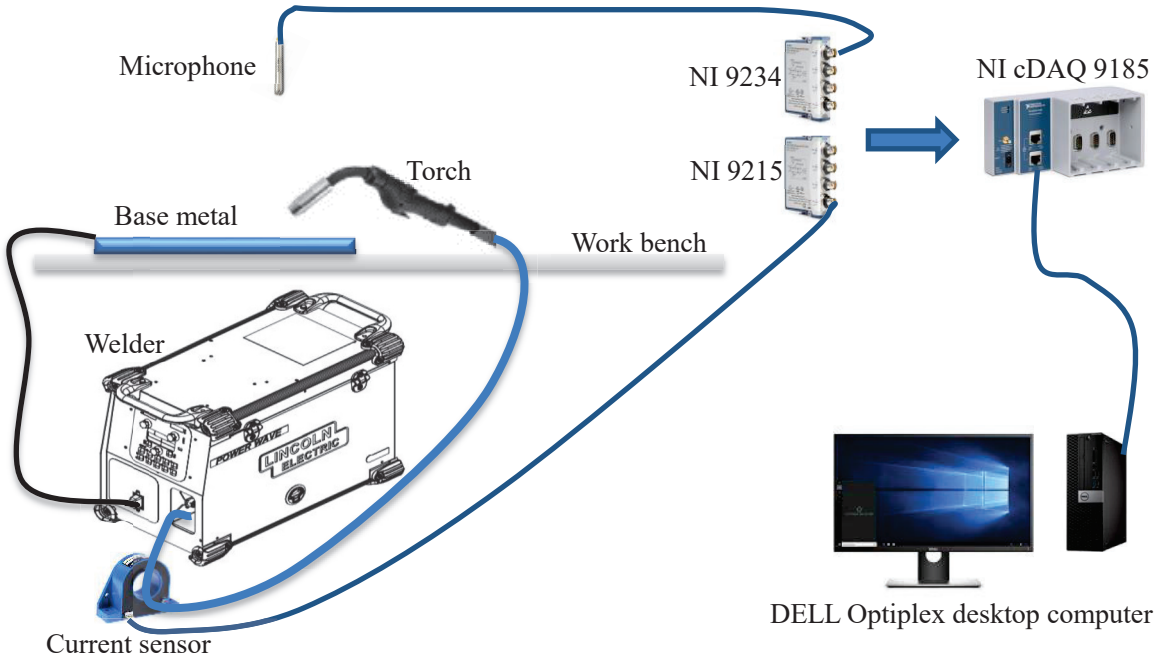

Figure 1 – Diagram of the experimental setup.

In GMAW, there are many different metal transfer modes, depending on various operational variables, such as the welding current, composition of shielding gas, electrode extension, ambient pressure, polarity and welding material (11,12). The welding current is the most used variable for the welders to adjust for obtaining the desired metal droplet transfer mode (12). Identifying the metal transfer mode is critical for process monitoring and quality control of GMAW (11). Therefore, the pure contact transfer and the pure free flight mode were produced in the experiments to investigate the statistical difference between the both. In addition to the natural GMAW, a Pulsed-GMAW mode was also performed in the experiments, where a controlled pulsed current waveform was used. Therefore, three metal transfer modes are studied in this paper which aligns with an academic weld droplet mode designation .

A software with a user interface is developed with LabWindows/CVI 2017 to acquire, display and store the signals in synchronisation. The sampling rate for the sound and current signals are 51.2 kHz and 3.2 kHz, respectively. The measured sound pressure and current signal are shown in Figure 2 for the pure contact transfer mode. The current signal shows that the welding current increases from a base value of approximately 85 A to a peak value of approximately 280 A first and then slumps to the base value. The increase in the current value shows the build-up of the droplet attached to the electrode while the peak current value corresponds to the short-circuiting phase of the contact metal transfer, where the droplet is big enough to connect the electrode to the base metal (13). The droplet detaches from the electrode to the base metal and the current slumps to the base value again, which is called the arcing phase (13). The process repeats and a sequence of current peaks is formed during the whole welding process.

Figure 2 demonstrates that an acoustic impulse is formed immediately after each current peak, indicating that the welding sound is produced by the quick energy release in the short-circuiting phase. The detailed sound generation mechanism is beyond the scope of this paper and will be investigated in future. In this paper, the statistical characteristics of the sound impulses are studied, e.g., the peak sound pressure in the impulses and the impulse interval as illustrated in Figure 2(a). In addition, the event duration is defined to describe the time length of the cycling that corresponds to the increase and decrease in the current value, as denoted by the green rectangle in Figure 2. The peak sound pressure, the impulse interval and the event duration can be calculated from the envelope of the sound signals, as depicted in the following section. The correspondence between the sound and current signals for other metal transfer modes are similar and not shown here for the sake of brevity.

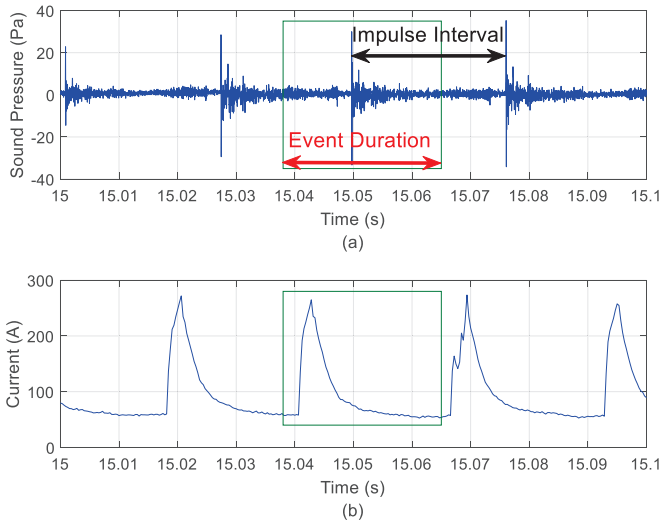

Figure 2 – (a) Sound pressure and (b) welding current measured during the contact transfer GMAW.

3. STATISTICAL ANALYSIS AND DISCUSSIONS

To calculate the peak sound pressure, impulse interval and event duration for the sound impulses in the sound signal, the envelope of the absolute sound pressure is first estimated. Figure 3(a) shows the sound signal for the pure contact transfer mode and Figure 3(b) illustrates the absolute sound signal with the estimated envelopes (red curve). The envelope refers to the smooth curve outlining the acoustic impulses in the welding sound signal. The peak value in the envelope denotes the peak sound pressure, the time interval between two consecutive peaks denotes the impulse interval, and the time period between two consecutive valleys denotes the event duration. To describe the statistical characteristics of these variables, the probability density function is estimated and fitted to various statistical distribution model. It was found that the Burr distribution shows excellent performance in fitting the probability density function. The Burr distribution is defined as (14)

$$f(x|\alpha,c,k) = \frac{kc(x/\alpha)^{c-1}}{\alpha[1+(x/\alpha)^{c}]^{k+1}} \quad (1)$$

where x is the variable and α, c and k are three positive function parameters.

3.1 Contact transfer mode

A typical sound signal for the contact transfer mode is shown in Figure 3(a) and the corresponding absolute sound pressure and the estimated envelope is illustrated in Figure 3(b). The histogram of the peak sound pressure is shown in Figure 4(a), which is not symmetric and cannot be modelled by a normal distribution. Instead, the Burr distribution can be used the fit the histogram very well, as shown by the red curve in Figure 4(a). Similarly, the distributions of the impulse interval and the event duration are also asymmetrical, as shown in Figure 4(b) and (c), respectively. The probability distributions of the impulse interval and the event duration are very similar because they are actually pertinent to each other, as shown in Figure 2(a).

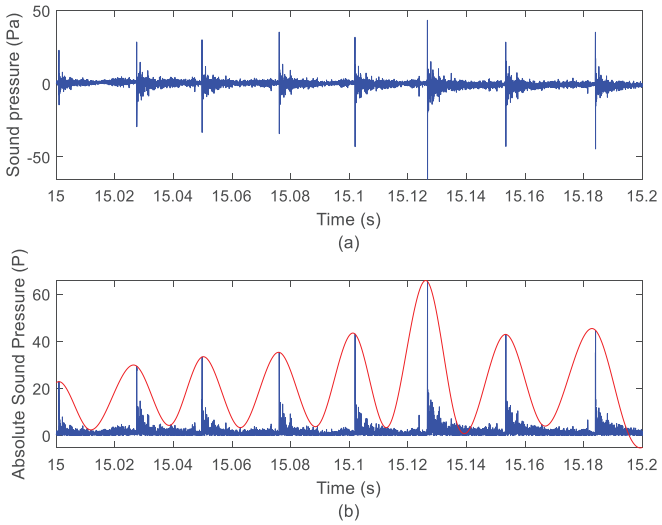

Figure 3 – (a) Measured sound pressure and (b) the estimated envelope on the absolute sound pressure.

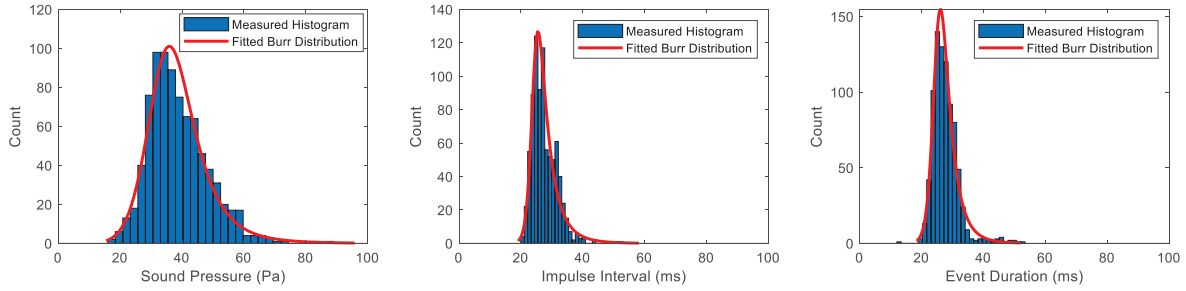

(a) (b) (c)

Figure 4 – Histogram and fitted Burr distribution for (a) sound pressure, (b) impulse interval and (c) event duration for the welding sound at short-circuiting mode.

To describe the asymmetry in the probability distribution, the skewness is calculated as (15)

$$s = \frac{E(x-\mu)^3}{\sigma^3} \tag{2}$$

where μ and σ denote the mean and standard deviation of the variable x, respectively, and E() denotes the expectation. A positive skewness indicates that the distribution is tailed to the right while a negative skewness depicts a tail on the left. The skewness of a perfect symmetrical distribution such as the normal distribution is zero.

The mean, standard deviation and the skewness of the peak sound pressure, the impulse interval and the event duration are shown in the first row of Table 1. The mean and standard deviation of the peak

sound pressure are 38.7 Pa and 9.5 Pa, respectively. The skewness is 0.8, indicating that the probability distribution is slightly tailed to the right, as shown in Figure 4(a). The mean and standard deviation of the impulse interval and the event duration are almost the same because they are pertinent as discussed above. The skewness of the impulse interval and the event duration is larger than that of the peak sound pressure, which stand for a longer tail to the right, as illustrated in Figures 4(b) and (c).

Table 1 – Statistics of the welding sound event based on the envelope estimation

Variables	Sound Pressure			Impulse Interval			Event Duration		
Statistics	μ	σ	s	μ	σ	s	μ	σ	s
Contact transfer	38.7	9.5	0.8	27.6	4.1	1.5	27.6	4.2	2.0
Free flight	8.6	4.8	2.9	32.7	9.9	1.7	32.6	10.3	1.5
Pulsed-GMAW	8.2	1.1	0.1	13.9	0.5	-0.1	13.9	0.8	0.0

3.2 Free flight mode

The typical sound signal for the pure free flight mode is shown in Figure 5(a) and the estimated envelope (red curve) of the absolute sound pressure is illustrated in Figure 5(b). By comparing Figure 5(b) with Figure 3(b), it is clear that the peak sound pressure level for the free flight mode is much lower than that for the contact transfer mode. In addition, the acoustic impulses are irregular as the impulse interval varies much with time. These differences can be clearly observed from the probability distribution, as shown in Figure 6.

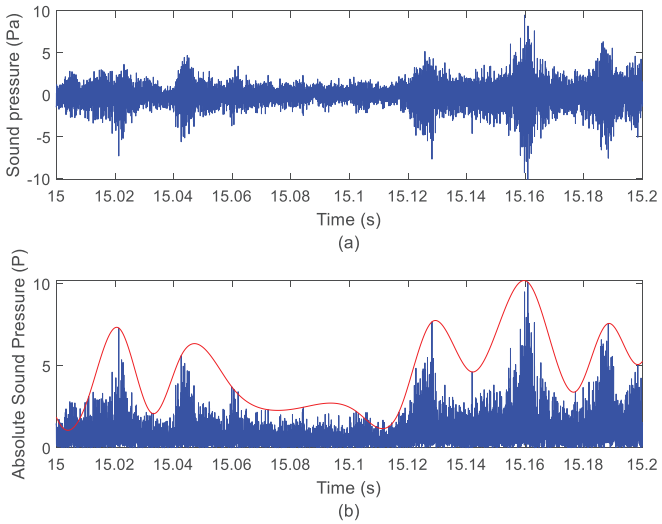

Figure 5 – (a) Measured sound pressure and (b) the estimated envelope on the absolute sound pressure.

Most of the peak sound pressure in Figure 6(a) is smaller than that in Figure 4(a) and the distribution is more heavily skewed to the right. This leads to a smaller mean value and a larger skewness compared to the peak sound pressure distribution for the contact transfer mode, as depicted in Table 1. On the other hand, the acoustic impulses are irregularly distributed, as evidenced by the waveform in Figure 5 and the wider distribution of the impulse interval and the event duration in Figure 6(b) and (c). This can be quantized by the standard deviation, as depicted in Table 1. The standard deviation is 9.9 and 10.3 for the impulse interval and the event duration at the free flight mode, which are much larger than that at the contact transfer mode.

In summary, the peak sound pressure of the free flight mode is much smaller than that of the contact transfer mode, and the acoustic impulses are irregularly distributed as evidenced by the larger standard deviation of the impulse interval and the event duration.

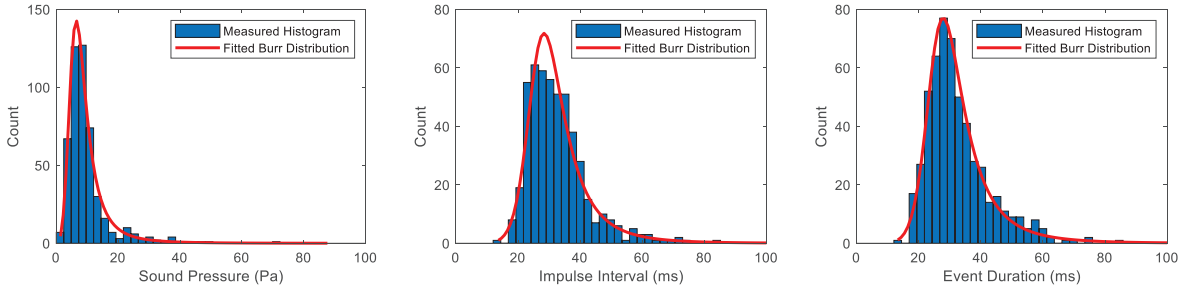

(a) (b) (c)

Figure 6 – Histogram and fitted Burr Distribution for (a) sound pressure, (b) impulse interval and (c) event duration for the welding sound at free-flight mode.

3.3 Pulsed-GMAW

Pulsed-GMAW is often used to improve weld quality as well as productivity in thin sheet metal industries (16). A Pulse-GMAW was also performed in the experiments at the pure contact transfer mode. The typical sound signal is shown in Figure 7(a) and the estimated envelope for the acoustic impulses is shown in Figure 7(b) based on the absolute sound pressure. It is clear that the acoustic impulses are very regularly distributed and the impulse interval is smaller than the contact transfer mode in Figure 3 and the free flight mode in Figure 5 under natural GMAW. The probability distribution of the peak sound pressure in Figure 8(a) shows that the sound pressure is concentrated to a very thin region, indicating the standard deviation is quite small. In addition, the distribution is almost symmetrical, so the skewness is as small as 0.1 as shown in Table 1.

Similarly, the probability distributions of the impulse interval and the event duration are also concentrated in a small region and almost symmetrical, so the standard deviation and the skewness are very close to zero, as depicted in Table 1. In addition, the mean impulse interval and event duration are smaller than that at the contact transfer mode and free flight mode under natural GMAW. These unique characteristics shed light on distinguishing the Pulsed-GMAW from the contact transfer mode and the free flight mode under natural GMAW based on sound signals.

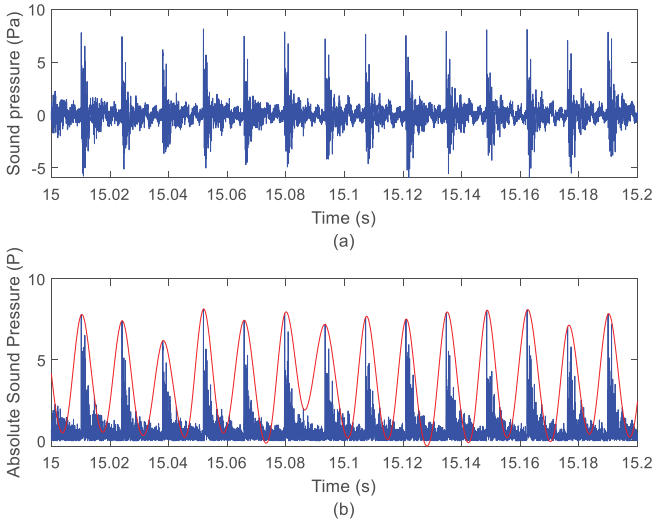

Figure 7 – (a) Measured sound pressure and (b) the estimated envelope on the absolute sound pressure.

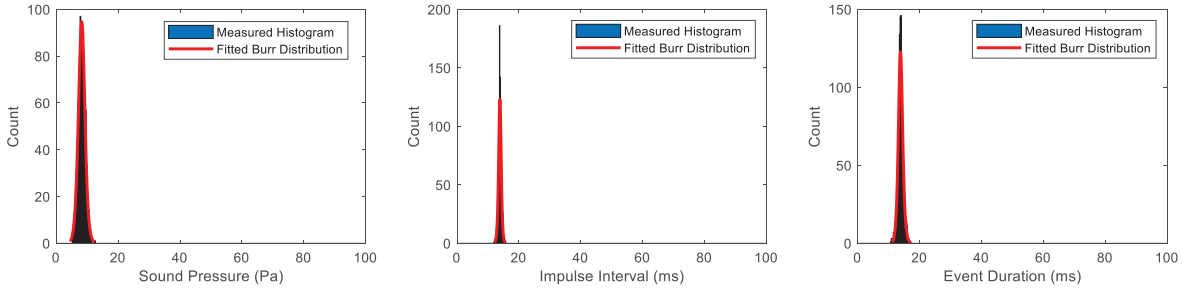

(a) (b) (c)

Figure 8 – Histogram and fitted Burr Distribution for (a) sound pressure, (b) impulse interval and (c) event duration for the welding sound at pulse mode.

In summary, the difference between different metal transfer modes in GMAW can be clearly seen from the statistical analysis of the welding sound signals, which consist of many acoustic impulses. In the welding sound recorded at the free flight mode, the impulses are irregularly distributed with time, as evidenced by the wide spread of the histograms of the impulse interval and event duration and the large value of the standard deviation. In contrast, in the welding sound produced by Pulsed-GMAW, the acoustic impulses are regular with an almost constant impulse interval, so the histograms of the impulse interval and the event duration are concentrated in a small region and the standard deviation is very small. The characteristics of the welding sound recorded at the contact transfer mode lie in between, but the peak sound pressure level is much higher than both the free flight mode and the Pulsed-GMAW.

In addition to the mean value, standard deviation and skewness, the model parameters of the Burr distribution in Equation (1) are also different for different metal transfer mode, as summarized in Table 2. The relationship between the model parameters and the shape of the histogram is not intuitive from Equation (1), but Table 2 shows clearly that the model parameters are remarkably different, as the histograms in Figures 4, 6 and 8. These different characteristics can be used as the dedicated features for welding sound signals to distinguish the metal transfer mode automatically, which will be investigated in a future work. The limitation of the current research is that the analysis is based on the clean welding sound. The effect of the background noise in the factory environment on the statistical characteristics of welding sound will be investigated in future.

Table 2 – Model parameters of the Burr distribution for different welding sound

Variables	Sound Pressure			Impulse Interval			Event Duration		
Parameters	α	c	k	α	c	k	α	c	k
Contact transfer	36.8	7.5	0.9	24.5	22.2	0.3	25.3	18.4	0.5
Free flight	7.9	3.7	1.1	27.1	9.1	0.5	26.7	8.5	0.5
Pulse-GMAW	8.8	10.5	1.8	13.9	48.1	1.2	13.9	29.8	1.0

4. CONCLUSIONS

This paper explores the statistical characteristics of the welding sound recorded at different metal transfer modes, which aims to find out the dedicated features for the welding sound to create a datum to automatically distinguish metal transfer modes. The probability distribution of the peak sound pressure, the impulse interval and the event duration were calculated based on the estimated envelope of the absolute sound signals and were found to be modelled well by the Burr distribution. Different characteristics of the welding sound at different metal transfer modes can be clearly observed from the shape of the histograms, the model parameters and the statistics such as the mean, standard deviation and skewness. These unique characteristics are promising to be used as the dedicated features for welding sound signals to distinguish the metal transfer mode automatically, which will be investigated in a future study. The physical generation mechanism of the welding sound at different metal transfer modes will

be investigated in the future.

ACKNOWLEDGEMENTS

This research is supported under the Australian Research Council's Linkage Project (No. LP160100616) and the UTS FEIT Tech Lab Blue Sky Grant.

REFERENCES

1. Tam J. Methods of Characterizing Gas-Metal Arc Welding Acoustics for Process Automation. University of Waterloo; 2005.
2. Pal K, Bhattacharya S, Pal SK. Investigation on arc sound and metal transfer modes for on-line monitoring in pulsed gas metal arc welding. J Mater Process Technol [Internet]. 2010 [cited 2019 Apr 8];210(10):1397–410. Available from: https://pdf.sciencedirectassets.com/271356/1-s2.0-S0924013609X00257/1-s2.0-S092401361000110X/main.pdf?x-amz-security-token=AgoJb3JpZ2luX2VjEHcaCXVzLWVhc3QtMSJHMEUCIQD64zBaJrKx2QwYalh02a98FpS%2BmhhS6kgp75Czgh74%2FwIgcXi2%2Be6YMBmzGRuGbKS2oQId0KAIChTttGKIDl
3. Jolly WD. Acoustic emission exposes cracks during welding. Weld J. 1969;48:21–7.
4. Saini BD, Floyd S. An investigation of Gas Metal Arc Welding sound signature for on-line quality control. Weld Res Suppl [Internet]. 1998 [cited 2016 Dec 11];(April):172–9. Available from: https://www.audiolabs-erlangen.de/resources/MIR/TSMtoolbox
5. Wang Y, Zhao P. Noncontact acoustic analysis monitoring of plasma arc welding. Int J Press Vessel Pip [Internet]. 2001 [cited 2018 Mar 31];78(1):43–7. Available from: https://ac.els-cdn.com/S0308016100000855/1-s2.0-S0308016100000855-main.pdf?_tid=dcf794e2-5c17-4823-a66e-7fbc36b5654e&acdnat=1522480341_9a06ae68e9f1fe0a5e85868c4e1c7572
6. Cayo EH, Alfaro SCA. GMAW process stability evaluation through acoustic emission by time and frequency domain analysis. J Achiev Mater Manuf Eng. 2009;34(2):157–64.
7. Ting YY, Hung KC, Tzeng YF. Wavelet Package for the In-Process Monitoring of Gas Metal Arc Welding Mild Steel. Appl Mech Mater [Internet]. 2011 Oct [cited 2016 Dec 11];121–126:3652–6. Available from: http://www.scientific.net/AMM.121-126.3652
8. Yusof MFM, Kamaruzaman MA, Ishak M, Ghazali MF. Porosity detection by analyzing arc sound signal acquired during the welding process of gas pipeline steel. Int J Adv Manuf Technol [Internet]. 2017 [cited 2018 Apr 9];89(9–12):3661–70. Available from: https://link.springer.com/content/pdf/10.1007%2Fs00170-016-9343-4.pdf
9. Sumesh A, Rameshkumar K, Mohandas K, Babu RS. Use of machine learning algorithms for weld quality monitoring using acoustic signature. In: Procedia Computer Science [Internet]. 2015. p. 316–22. Available from: www.sciencedirect.com
10. Lv N, Xu Y, Li S, Yu X, Chen S. Automated control of welding penetration based on audio sensing technology. J Mater Process Technol [Internet]. 2017 [cited 2018 Apr 9];250:81–98. Available from: www.elsevier.com/locate/jmatprotec
11. Zhao S, Qiu X, Burnett I, Rigby M, Lele A. GMAW metal transfer mode identification from welding sound. In: Proceedings of Acoustics 2018. 2018. p. 1–10.
12. Kim YS, Eagar TW. Analysis of Metal Transfer in Gas Metal Arc Welding. Weld J [Internet]. 1993 [cited 2018 Apr 6];1:269s–278s. Available from: http://eagar.mit.edu/Publications/Eagar117.pdf
13. Wang Y, Lü X, Jing H. Dynamic simulation of short-circuiting transfer in GMAW based on the "mass-spring" model. Int J Adv Manuf Technol [Internet]. 2016 [cited 2018 Apr 6];87(1–4):897–907. Available from: https://link.springer.com/content/pdf/10.1007%2Fs00170-016-8538-z.pdf
14. Tadikamanlla PR. A look at the Burr and related distributions. Int Stat Rev. 1980;48(3):337–44.
15. Joanes DN, Gill CA. Comparing Measures of Sample Skewness [Internet]. Vol. 47, Journal of the Royal Statistical Society. Series D (The Statistician). 1998 [cited 2019 Apr 15]. Available from: https://www-jstor-org.ezproxy.lib.uts.edu.au/stable/pdf/2988433.pdf?ab_segments=0%2Fdefault-2%2Fcontrol&refreqid=search%3Aec0fafd916073adc91cfb330aae2daf5
16. Zhao Y, Chung H. Influence of power source dynamics on metal and heat transfer behaviors in pulsed gas metal arc welding. Int J Heat Mass Transf [Internet]. 2018 [cited 2019 Feb 18];121:887–99. Available from: https://doi.org/10.1016/j.ijheatmasstransfer.2018.01.058